New Understanding of Tokamak Plasma Response to 3D Magnetic Fields

J.-K. Park 1), J. E. Menard 1), M. J. Schaffer 2), A. H. Boozer 3), R. J. Hawryluk 1), Holger Reimerdes 3), T. Evans 2), the NSTX Research Team and DIII-D Research Team

1) Princeton Plasma Physics Laboratory, Princeton, New Jersey, USA
2) General Atomics, P. O. Box 85608, San Diego, California 92186, USA
3) Columbia University, New York, New York, USA

e-mail contact of main author: jpark@pppl.gov

Abstract. The performance of both present and future tokamaks such as ITER can be greatly degraded or enhanced by small 3D magnetic perturbations. An important new tool for understanding 3D magnetic field effects in tokamaks is the Ideal Perturbed Equilibrium Code (IPEC), which computes 3D perturbed tokamak equilibria including plasma response effects such as poloidal harmonic coupling, shielding, and amplification. IPEC predictions have been verified by recent error field correction results on NSTX and DIII-D, where the strong plasma response effects are essential to explain observed Locked Mode (LM) behavior. Also, a generalized Neoclassical Toroidal Viscosity (NTV) theory in tokamaks indicates that the variation of field strength predicted by IPEC, including effects of the deformed flux surfaces, is consistent with the experimentally measured rotational damping rates. Based on these results, IPEC has been used to characterize Resonant Magnetic Perturbation (RMP) for Edge Localized Mode (ELM) suppression, and to optimize ITER RMP field. The initial results show that the optimization of three rows of coils (two off-midplane rows and one midplane row) can give a great benefit to RMP by minimizing core degradation toward a theoretical minimum level.

1. Introduction

Tokamak plasmas respond sensitively to externally driven 3D magnetic fields. An external field as small as $\delta B^x / B \sim 10^{-4}$ can greatly change the performance of plasmas by causing plasma locking [1-3], rotational damping [4, 5] by non-ambipolar transport [6-8]. In order to understand such sensitive plasma responses, a precise description of plasma equilibria would be required as typical in 2D tokamak problems. The Ideal Perturbed Equilibrium Code (IPEC) [9] has been developed for the purpose, based on DCON [10] and VACUUM [11] stability code, since perturbed equilibria [12] are essentially the same subject as plasma stability. What has been shown by IPEC is the existence of strong plasma response effects - poloidal harmonic coupling, shielding and amplification of the field and the displacement. Recent error field correction results on NSTX and DIII-D highlighted the importance of the plasma response effects to explain observed locked mode (LM) behavior with the resonant field [13]. Another important consequence by 3D magnetic fields is the non-ambipolar transport and the resulting toroidal torque, which is often termed Neoclassical Toroidal Viscoscity (NTV) effect in tokamaks [8]. The NTV theory has been recently generalized for tokamaks and it is shown that the IPEC prediction for the deformations of the flux surfaces may be also essential to explain observed torque and rotational damping [14]. Based on these studies, the resonant field and NTV torque predicted by IPEC are used to characterize Resonant Magnetic Perturbation (RMP) [15-17] required for the suppression of Edge Localized Mode (ELM). The IPEC characterizations are applied to the optimization of RMP field using ITER coils. In this paper, IPEC will be introduced in section 2, the validation and implication of plasma response effects will be described in section 3, IPEC characterization and optimization of ITER RMP field will be illustrated in section 4 followed by final remarks in section 5.

2. Ideal Perturbed Equilibrium Code (IPEC)

2.1. Development of IPEC

IPEC [9] finds 3D perturbed scalar pressure equilibria with shielded islands in tokamaks. Given a 2D tokamak equilibrium and an externally driven 3D field, an ideal perturbed equilibrium can be determined by solving the ideal force balance $\vec{\nabla}\delta p = \vec{j}\times\delta\vec{B}+\delta\vec{j}\times\vec{B}$ with boundary conditions set by external coils, while preserving the pressure $p(\psi)$ and the safety factor $q(\psi)$ profiles. Since a fixed-boundary problem can be exactly solved by a stability code if the kinetic energy is properly suppressed, IPEC augments DCON [10] and VACUUM [11] stability codes to solve the force balance given a set of perturbed field distributions $\delta\vec{B}\cdot\vec{n}_b$ on the plasma boundary. A free-boundary problem can be solved using virtual surface currents on the boundary to match a set of $\delta\vec{B}\cdot\vec{n}_b$ with a given external field $\delta\vec{B}^x\cdot\vec{n}_b$ which can be found by superposing vacuum field on the plasma boundary. Thus, the *total field* $\delta\vec{B}\cdot\vec{n}_b$ can be found using $\delta\vec{B}\cdot\vec{n}_b=\hat{P}\,[\delta\vec{B}^x\cdot\vec{n}_b]$, with a permeability operator $\hat{P}$, if an *external field* $\delta\vec{B}^x\cdot\vec{n}_b$ is given on the plasma boundary.

2.2. Features in ideally perturbed equilibria

Since ideally perturbed equilibria assume the perfect shielding of islands, there is no resonant field at the rational surfaces, but the jump of tangential field exists and produces the shielding currents as [12]

$$\vec{j}_{smn}=\Delta_{mn}\frac{ime^{i(m\theta-n\varphi)}}{\mu_0 n^2(\oint dSB^2/|\nabla\psi|^3)}\delta(\psi-\psi_{mn})\vec{B},\ \text{where}\ \ \Delta_{mn}\equiv\left[\frac{\partial}{\partial\psi}\frac{\delta\vec{B}\cdot\vec{\nabla}\psi}{\vec{B}\cdot\vec{\nabla}\varphi}\right]. \qquad (1)$$

The shielding current produces a field equal and opposite to the field driving an island. This *total resonant field* $\delta B_{mn}\equiv(\delta\vec{B}\cdot\vec{n})_{mn}$, which is approximately proportional to the shielding current, includes the self-consistent ideal plasma response and is distinct from the *external resonant field* $\delta B^x_{mn}\equiv(\delta\vec{B}^x\cdot\vec{n})_{mn}$ superposed in vacuum.

Shielded islands imply that the flux surfaces are not destroyed, but deformed in IPEC equilibria. Since the variation of the field strength seen by particles is the field seen on these deformed flux surfaces [18], the true variation of the field strength divided by B_{T0} is $\delta=\delta_E+(\vec{\xi}\cdot\vec{\nabla}B)/B_{T0}$, where $\delta_E=(\delta\vec{B}\cdot\hat{b})/B_{T0}$ is the *Eulerian* variation at a fixed spatial point. The variation δ can be compared to δ^x_E, which is the Eulerian variation evaluated using vacuum field as has been typically used as an approximation. Note that the dominant difference occurs between δ and δ_E, not between δ_E and δ^x_E. The variation δ_E in IPEC has the similar amplitude to the variation δ^x_E in vacuum, if the plasma amplification is weak.

3. Importance of Plasma Response Effects

3.1 Plasma Locking and Resonant Field

What determines locking physics is the shielding current, or equivalently, the total resonant field δB_{mn}. Previous attempts to mitigate plasma locking by correcting the intrinsic error

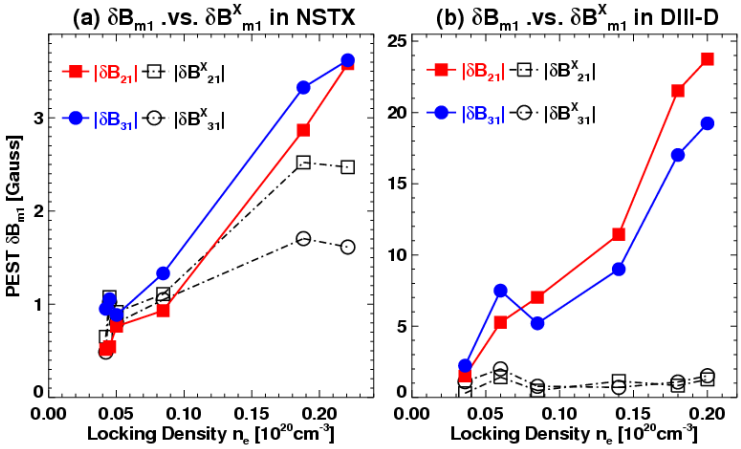

Fig.1 *Comparison between* δB_{mn} *and* δB^{x}_{mn} *at the rational surfaces as functions of critical density in (a) NSTX (b) DIII-D locking experiments.*

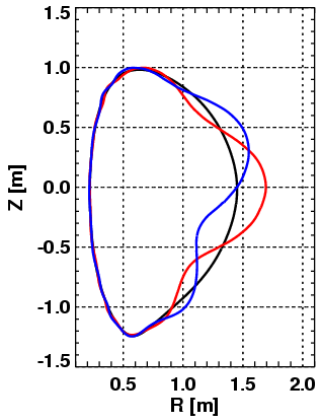

Fig.2 *The most sensitive external field on the plasma boundary,* $\delta\vec{B}^{x}\cdot\hat{n}_{b}=A(\theta)\cos\varphi+B(\theta)\sin\varphi$ *, in NSTX, where red line is* $A(\theta)$ *and the blue line is* $B(\theta)$*.*

field using correction coils have been based δB^{x}_{mn} as an approximation, but often give misleading results. Fig. 1 shows the correlations using δB_{mn} and δB^{x}_{mn} with locking density in NSTX and DIII-D experiments [13]. Since a variety of experiments has given evidence that the locking density is linearly correlated with the strength of 3D field [1-3], the results with δB^{x}_{mn} were contrary to experiments. The linear correlations are restored when the correct IPEC δB_{mn} is used. These experiments were performed in low β Ohmic plasmas, but recent error field experiments in DIII-D indicate that IPEC predictions are also consistent with observations in high β NBI plasmas [19]. The IPEC analysis is expected to be a good approximation as long as perturbed potential energy δW is greater than and reasonably far from zero, which is the marginal point for the given external perturbation.

Another important result is that the two different δB_{mn} at $q=2,3$ rational surfaces show a similar amplification, which implies that the plasma response is dominated by a single distribution of the external field. *The most sensitive field* can be found using Singular Value Decomposition (SVD) for the coupling matrix $\vec{\vec{C}}$ between the total resonant field and the external field decomposed on the boundary [20]. Fig. 2 shows how the most sensitive external field looks on the plasma boundary in NSTX. The most sensitive field is very robust spanning a wide range of plasma parameters and explains why the outboard coils can be effective for mitigating the intrinsic error field.

3.2. Variation of Field Strength and NTV Torque

The 3D perturbations cause non-ambipolar diffusion and torque, which have been studied by Shaing for different regimes [8, 21] in tokamaks. This is so-called NTV theory and has been tested in NSTX [4] and DIII-D [5]. The NTV torque is proportional to a weighted square of the variation in the field strength $\delta_{w}^{2}=\sum_{mm'}W_{mm'}\delta_{nm}\delta_{nm'}$, where $W_{mm'}$ is a weighting factor given by bounce integrations, which depends on the regime, and the δ_{nm}'s are the Fourier

harmonics of δ. To determine the δ_{nm} self-consistently, one needs to include the currents δj_{Π} associated with the torque T_φ in the calculation of perturbed equilibria. The present form of IPEC includes only the currents δj_p associated with the scalar pressure, however, one can use IPEC as an approximation if $\delta j_p >> \delta j_{\Pi}$, or equivalently, $s \equiv -\delta W / \delta W_v \gg \alpha \equiv T_\varphi / 2n\delta W_v$ [22], where δW is the perturbed energy and δW_v is the perturbed energy in vacuum. It is found that $s \gg \alpha$ for most of practical external perturbations, except $n=1$ applications to high β plasmas [23]. When IPEC is used for $\delta = \delta_E + \vec{\xi} \cdot \vec{\nabla} B / B_{T0}$, it has been found that typically $\delta \approx 10^{-3}$, when $\delta_E^x \approx 10^{-4}$ in practice.

The previous study shows that $\delta_E^x \approx 10^{-4}$ is a sufficient amplitude to explain observations if a plasma is in purely $1/\nu$ regime, where the toroidal precession is ignored [4, 24]. However, it has been recently noticed that even $\delta \approx 10^{-3}$ is not sufficient to explain observations if the precession is precisely included [14, 25]. In order to resolve the inconsistent prediction in theory, a general formula has been derived connecting regimes and also including bounce harmonic resonances [14]. For the particles precessing ℓ times of the full toroidal angle during one bounce, the toroidal torque is given by

$$\left\langle \phi \cdot \nabla \cdot \Pi^{\ell} \right\rangle = \frac{\varepsilon^{1/2} p}{\sqrt{2}\pi^{3/2}} \left\langle \frac{1}{R} \right\rangle \int_0^1 d\kappa^2 \delta_w^{2,\ell} \int_0^\infty dx R_1^{\ell} \left(u^{\varphi} + 2\sigma \left| \frac{1}{e} \frac{dT}{d\chi} \right| \right), \tag{2}$$

where the weighted square of the variation of field strength is

$$\delta_w^{2,\ell} = \sum_{nmm'} \left(Re(\delta_{nm}) Re(\delta_{nm'}) + Im(\delta_{nm}) Im(\delta_{nm'}) \right) \frac{F_{nmlc}^{-1/2} F_{nm'lc}^{-1/2}}{4K(\kappa)}, \tag{3}$$

and the resonant term

$$R_1^{\ell} = \frac{1}{2} \frac{n^2 (1 + (\ell/2)^2/2)(\nu/2\varepsilon)}{\left[\ell\omega_b - n(\omega_E + \omega_B) \right]^2 + \left[(1 + (\ell/2)^2)(\nu/2\varepsilon) \right]^2 x^{-3}}. \tag{4}$$

Here ε is the inverse aspect ratio, p is the pressure, R is the major radius, u^{φ} is the angular frequency of toroidal rotation, σ is the sign function that +1 for co-rotation, T is the temperature, χ is the poloidal flux divided by 2π, K is the complete elliptic integral of the first kind, κ is the normalized pitch, and $x = E/T$ with particle energy E. The function F is defined as $F_{nmlc}^{y} = \int_{-\theta_t}^{\theta_t} d\theta (\kappa^2 - \sin^2(\theta/2)) \cos\left[(m - nq - \sigma\ell)\theta \right]$ with the turning point $\theta_t = \arcsin(\kappa)$. The bounce frequency $\omega_b = (\pi/4\sqrt{2})\omega_t \sqrt{\varepsilon x}$, the electric toroidal precession $\omega_E = d\phi_e / d\chi$ and the magnetic toroidal precession $\omega_B = \sigma q^3 \omega_t^2 x / 4\varepsilon\omega_g$ with the transit frequency $\omega_t = v_t / qR_0$ and the gyro-frequency $\omega_g = eB/M$. What dominates the transport is the small fraction of resonant particles, $\ell\omega_b - n(\omega_E + \omega_B) \approx 0$, which are effectively in $1/\nu$ regime.

The Fig. 3 shows the damping rates given by Eq. (2) when $\delta \approx 10^{-3}$ and practical parameters are used. The parameters are chosen to model the core region in DIII-D, but also can model other devices by a scaling $\nu_{damp} \propto 1/R_0^2$. One can see 10~100/s damping rates for $\nu_{ii} = 10^3 \sim 10^4$ /s and for the rotational frequency $f = 10kHz$. Also, it gives the $1/\nu$ parametric dependency for $\nu_{ii} = 10^3 \sim 10^4$, even though plasmas would be in ν regime if a

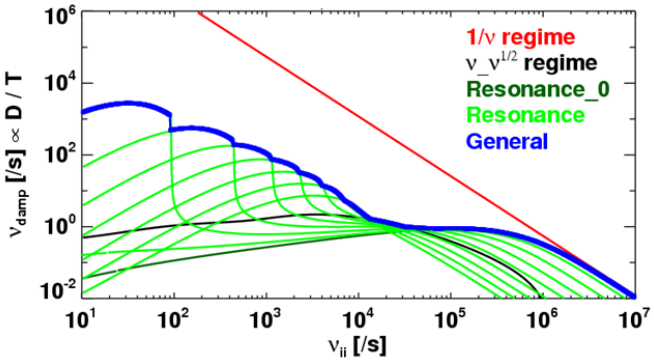

Fig.3 *Rotational damping rates as a function of ion-ion collision frequency evaluated by each formula in* $1/\nu$ *regime [8],* $\nu\_\nu^{1/2}$ *regime [21], and general formula including each resonance (*$\ell = 0$, *Resonance_0 and* $\ell > 0$, *Resonance) [14]. Parameters are* $R_0 = 2m$, $\varepsilon = 0.3$, $q = 2.2$, $n_e = 5\times10^{19} m^{-3}$, $\omega_E / 2\pi = f_\phi = 10^4$, $n = 3$, *and* $\delta_{mn} = 10^{-3} e^{-(m-5)^2/50}$.

simple criterion is used, that is, $\nu/\varepsilon < \omega_E$. These results are consistent with observations [4, 5], which were not consistent with the previous theory. Note that the bounce harmonic resonances enhance the NTV torque by $\sim 10^2$ factor compared to the estimations for $\ell = 0$ and $\nu\_\nu^{1/2}$ regime, and also δ/δ_E^x enhances the torque by $\sim 10^2$ factor. Other parameters make the varation of the torque more complicated, but are almost ignorable compared to the two dominating factors. This strongly implies that IPEC evaluations giving $\delta \approx 10^{-3}$ may be essential to explain the observed damping rates.

4. Optimization of RMP in ITER

4.1 IPEC Characterization of RMP field

The suppression of ELMs by RMP, which was found on DIII-D [15-17], is an important issue on ITER. Since the installations of RMP coils in ITER are technically demanding, it is important to evaluate the potential benefits. Empirically if the RMP field provides the external field resonating with the edge magnetic field, possibly ergodizing the edge and enhancing particle transport, ELMs tend to be suppressed. Experimental ELM suppression correlates with having the Chirikov > 1 at $\psi_N \approx 0.85$. This *Chirikov condition* appears to be a necessary, but not a sufficient condition, and physics behind RMP with ELMs is not fully understood yet. The purpose of this study is to revisit RMP effects on plasmas using IPEC to include ideal plasma response effects. The two main features described in Section 2 and 3 are investigated : {1} the total resonant fields, or Chirikov parameters, and {2} weighted squares of variation in field strength, or NTV forces and rotational damping rates.

The Fig. 4 (a) shows the Chirikov parameters calculated using IPEC δB_{mn} for several DIII-D experimental discharges with various $n = 3$ RMP configurations. In these experiments, the C-coil did not suppress ELMs while each of the I-coil cases did suppress ELMs. Thus, as seen from Fig. 4 (a) when the plasma response is included, the Chirikov parameters can provide a necessary condition similar to the vacuum Chirikov condition, but not a sufficient condition for determining whether ELM suppression can be obtained with a particular set of RMP coils. Note that the IPEC Chirikov parameters for the C-coil case may not strictly meet the vacuum Chirikov condition [16], but are not so distinct from the I-coil cases. Moreover, the IPEC

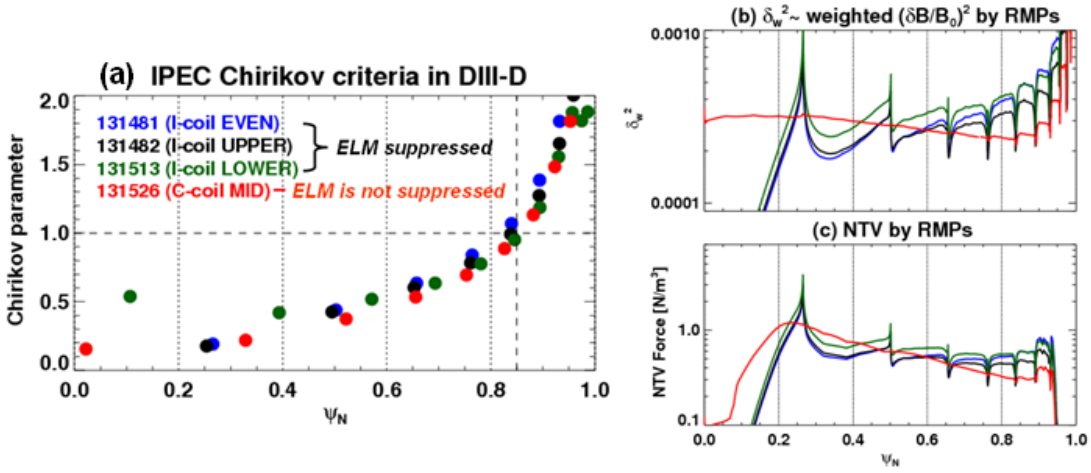

Fig.4 *Characterization of RMPs for ELM suppression. (a) IPEC Chirikov parameters, (b) Weighted* $\delta_w^{2,\ell=0}$ *by Eq. (3), and (c) NTV torque by Eq. (2) using a set of DIII-D transport parameters (t=3.15s, #127744) for four shots using different RMP configurations. Note that (a)~(c) includes ideal plasma response effects from IPEC.*

analysis for recent NSTX RMP experiments using the midplane coils also confirmed that the Chirikov condition is not sufficient [25]. As pointed out in [16], the Chirikov condition provides a convenient order parameter for size of the ELMs versus the applied RMP, but additional information is needed to determine physics involved. The variation in the field strength and corresponding NTV force, in Fig. 4 (b) and (c), may be one possibility. The weighted square δ_w^2 in Eq. (3) shows that the field by C-coil is very different due to the large ratios of non-resonant components to near-resonant components in the field. The NTV forces using the generalized Eq. (2) are almost proportional to δ_w^2 as can be seen with the fixed transport parameters. This implies that ELMs may be suppressed when RMP provides sufficient NTV transport. The NTV strongly affects the transport of particles, so it may be not so surprising that RMP experiments have shown the change of the density profiles, not the temperature profiles. Based on these characterizations, one can define the optimized field that {1} satisfies Chirikov condition, {2} and enhances NTV transport as more as possible in the edge, but {3} as little as possible in the core. Note that these three conditions are similar to the proposed design requirements for RMP coils [26], but do not include the *Pitch-alignment condition*, which remains the future work with IPEC.

4.2 Optimization of RMP for ITER

The optimization of the field using the three conditions requires the investigations of NTV torques with various spectra of the field. Since it is computationally demanding, here an approximate method is used, using the total resonant field δB_{mn} at the rational surfaces. Considering $\psi_N < 0.8$ as the core region and $\psi_N > 0.8$ as the edge region, one can find an edge-optimized field in terms of the external field on the boundary that maximizes $\sum |\delta B_{mn}|^2 / \sum \left| (\delta \vec{B}^x \cdot \hat{n}_b)_{mn} \right|^2$ in the edge, but minimize it in the core using SVD techniques. The *coil-optimized field* using a given set of coils can be found by seeking a combination of the coil currents that most effectively drive the theoretical *edge-optimized field*.

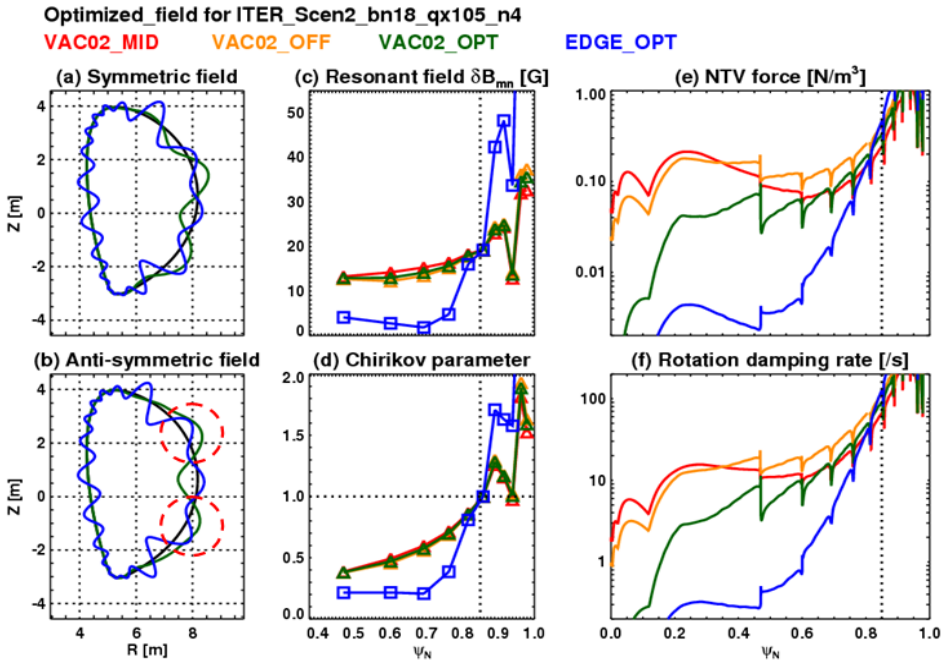

Fig.5 *Optimized results using midplane coils (VAC02_MID), two rows of off-midplane coils (VAC02_OFF), and all three rows (VAC02_OPT) for n=4 RMP field to an ITER inductive plasma. The edge-optimized results (EDGE_OPT) are also shown for comparison: (a) and (b) are the two components of* $\delta\vec{B}^x \cdot \hat{n}_b = A(\theta)\cos\varphi + B(\theta)\sin\varphi$ *for the coil-optimized and the edge-optimized field, (c) Total resonant field, (d) IPEC Chirikov parameters, (e) NTV forces and (f) rotational damping rates by NTV braking. The amplitudes are normalized by Chirikov=1 at* $\psi_N = 0.85$.

The RMP coils in ITER have been designed similarly to DIII-D, so two rows of off-midplane coils and one row of midplane coils are considered [26] and are designated as *VAC02* coils. In the optimization, the two off-midplane coils are serially connected (even configuration), so the free variables are the two amplitudes for off-midplane coils and midplane coils, and the relative toroidal phase between them. When the three variables are optimized, one can compare the resulting resonant fields or Chirikov parameters, and NTV forces or damping rates with the results by separate applications of the off-midplane and midplane coils, and also by the theoretical edge-optimized field. Fig. 5 shows the results using $n = 4$ RMP to the standard ITER inductive target plasma [24, 27]: (a) and (b) shows how the optimized field looks on the boundary in terms of the external field. The edge-optimized field is highly wiggly to create strong resonances in the edge, but the coil-optimized field approximates a part of the edge-optimized field on the outboard side as can be seen in red circles in (b), as a result of cancellations between the field by off-midplane and midplane coils. (c) and (d) shows the resonant fields and Chirikov parameters in each case. Note that the coil currents are set by Chirikov=1 at $\psi_N = 0.85$. The coil-optimized field does not improve the resonant fields or the Chirikov parameters in (c) and (d), but it does substantially improve NTV parameters as can be seen in (e) and (f). One can see that the coil-optimized field reduces rotational damping in core up to a factor of ~10. This result is obtained using an approximate optimization with δB_{mn}, but still illustrates well the potential benefits of the three rows of coils and the optimization. A better optimization will be studied in the future using the NTV parameters, and by allowing the two rows of the off-midplane coils to have independent currents.

5. Final Remarks

The ideal perturbed equilibria using IPEC showed the strong plasma response effects. Plasma locking experiments in NSTX and DIII-D verified the expectations. The NTV damping rates, based on the newly generalized NTV calculations, imply that the true variation of field strength on deformed flux surfaces in IPEC may be essential to explain observed rotational damping. Based on these results, IPEC is used to characterize RMP field required to suppress ELMs. The study shows that the optimization of the field can be achieved if the field maximizes perturbations in edge, but minimizes perturbations in core, and shows that three rows of coils can produce the great benefit by the optimization.

Acknowledgment

The authors would like to thank S. A. Sabbagh, A. M. Garofalo and M. Becoulet for useful discussions. This work was supported by the US department of Energy under contract DE-AC02-76CH03073 (PPPL), DE-FG02-03ERS496 (CU), and DE-FC02-04ER54698 (GA).

References

[1] Hender, T. C., et al., Nucl. Fusion 32 (1992) 2137
[2] La Haye, R. J., et al., Phys. Fluids B 4 (1992) 2098
[3] Wolfe, S. M., et al., Phys. Plasmas 12 (2005) 056110
[4] Zhu W., et al., Phys. Rev. Lett. 96 (2006) 225005
[5] Garofalo, A. M., et al., "Observation of Plasma Rotation Driven by Static Non-axisymmetric Magnetic Fields in a Tokamak, to be published in Phys. Rev. Lett. (2008)
[6] Boozer, A. H., Phys. Fluids 23 (1980), 2283
[7] Linsker, R., et al., Phys. Fluids 25 (1982) 143
[8] Shaing, K. C., Phys. Plasmas 10 (2003) 1443
[9] Park, J.-K., Phys. Plasmas 14 (2007) 052110
[10] Glasser, A. H., et al., Bull. Am. Phys. Soc. 42 (1997) 1848
[11] Chance, M. S., Phys. Plasmas 4 (1997) 2161
[12] Boozer, A. H., et al., Phys. Plasmas 13 (2006) 102501
[13] Park, J.-K., et al., Phys. Rev. Lett. 99 (2007) 195003
[14] Park, J.-K., et al., "Non-ambipolar Transport by Trapped Particles in Tokamaks", to be submitted (2008)
[15] Evans, T. E., et al., Phys. Rev. Lett. 92 (2004) 235003
[16] Fenstermacher, M. E., et al., Phys. Plasmas 15 (2008) 056122
[17] Evans, T. E., et al., Proc. 22nd Int. Conf. on Fusion Energy, Vienna, IAEA (2008)
[18] Boozer, A. H., Phys. Plasmas 13 (2006) 044501
[19] Reimerdes, H., et al., Proc. 22nd Int. Conf. on Fusion Energy, Vienna, IAEA (2008)
[20] Park, J.-K., et al., Nucl. Fusion 48 (2008) 045006
[21] Shaing, K. C., et al., Phys. Plasmas 15 (2008) 082506
[22] Boozer, A. H.,et al. Phys. Rev. Lett. 86 (2001) 5059
[23] Park, J.-K., et al., "Shielding of External Magnetic Perturbations by Torque in Tokamaks", submitted to Phys. Rev. Lett. (2008)
[24] Becoulet, M., et al., Proc. 22nd Int. Conf. on Fusion Energy, Vienna, IAEA (2008)
[25] Canik, J. M., et al., Synopsis, 22nd Int. Conf. on Fusion Energy, Vienna, IAEA (2008)
[26] Hawryluk, R. J., et al., Proc. 22nd Int. Conf. on Fusion Energy, Vienna, IAEA (2008)
[27] Ikeda, K., Nucl. Fusion 47 (2007) S1